Article

pubs.acs.org/Biomac

Effects of Synthetic Biomacromolecule Addition on the Flow Behavior of Concentrated Mesenchymal Cell Suspensions

Benoît G. C. Maisonneuve,[†,∥,⊥,#] Denis C. D. Roux,[∥,⊥,#] Peter Thorn,[‡] and Justin J. Cooper-White*[,†,§,○]

[†]Tissue Engineering and Microfluidics Laboratory, Australian Institute for Bioengineering and Nanotechology, [‡]School of Biomedical Science, [§]School of Chemical Engineering, The University of Queensland, St. Lucia, Queensland 4072, Australia

[∥]Laboratoire de Rhéologie et Procédés, UMR5520 UJF−Grenoble INP, CNRS, BP53, F-38041 Grenoble Cedex 9, France

[⊥]Université Joseph-Fourier Grenoble 1, BP 53, F-38041 Grenoble Cedex 9, France

[#]Université de Grenoble Alpes, Domaine Universitaire, F-38402 Saint Martin d'Hères Cedex, France

[○]CSIRO, Manufacturing Flagship, Clayton, Victoria 3168, Australia

ABSTRACT: In the fields of tissue engineering and regenerative medicine, many researchers and companies alike are investigating the utility of concentrated mesenchymal stem cell suspensions as therapeutic injectables, with the hope of regenerating the damaged tissue site. These cells are seldom used alone, being instead combined with synthetic biomacromolecules, such as branched poly(ethylene glycol) (PEG) polymers, in order to form cross-linked hydrogels post-injection. In this article, we present the results of a detailed experimental and analytical investigation into the impacts of a range of eight-arm PEG polymers, each presenting functional end groups, on the rheological properties of concentrated living cells of mesenchymal origin. Using two-photon confocal microscopy, we confirmed that the aggregates formed by the cells are fractal structures, the dimension of which changed with PEG polymer type addition. From these results and the observed substantial variation in rheological footprint with increasing volume fraction and different PEG polymer type, we propose a number of mechanisms driving such structural changes. Lastly, we derived a modified Krieger−Dougherty model to produce a master curve for the relative viscosity as a function of volume fraction over the range of conditions investigated (including shear stress and PEG polymer type), from which we extract the adhesion force between individual cells within these concentrated suspensions. The outcomes of this study provide new insights into the complex interactions occurring in concentrated mesenchymal cell suspensions when combined with synthetic biomacromolecules commonly used as precursors in tissue engineering hydrogels, highlighting their substantial impacts on the resultant rheological footprint.

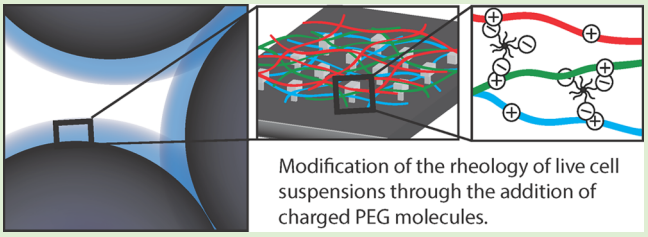

Modification of the rheology of live cell suspensions through the addition of charged PEG molecules.

INTRODUCTION

Suspensions of biologically derived materials, such as biopolymer microgels, are commonly used in foods and pharmaceutical formulation and have for many years been the focus of many rheological and structural investigations. Another biological suspension, blood, has similarly been the focus of much research in terms of it rheological behavior and flow properties. More recently, attention has turned to the flow behavior of other cell types, including a few studies of cells of mesenchymal tissue origin.[1,2] This is closely linked with the development of research areas such as bioengineering, tissue engineering, regenerative medicine and cellular therapy. Indeed, several applications and processes related to these fields have concentrated cellular suspensions as a core material. Knowing, understanding, and engineering the mechanical properties of cell suspensions in the absence and presence of soluble proteins and biomacromolecules has become crucial for the development and upscaling of these processes.

Most of the previous studies on the influence of polymer addition to concentrated suspensions have focused on non-biological and dimensionally small (hundreds of nanometers) systems, such as colloids; however, many of the observed behaviors may still be applicable to noncolloidal systems. When a macromolecule is added to a colloidal suspension, several behaviors can be observed, depending on the net interaction among the particles, the macromolecules, and the solvent.[3−6] If the particles are fully covered by the adsorbed polymer, then the interaction is mainly repulsive, and the suspension is then said to be sterically stabilized.[7,8] The origin of this interaction is believed to be due to the fact that the overlap of the polymer layers reduces the volume available to each single chain, increasing the free energy and hence producing a repulsive force.[7,9] In the case of attractive interactions, two mechanisms have been identified: bridging and depletion. If the polymer chains are able to be adsorbed onto the particle surfaces and if there are some free binding sites on the opposite surface, then

Received: October 5, 2014
Revised: December 2, 2014
Published: December 3, 2014

bridging can occur.[4] This interaction exponentially decreases with a characteristic distance on the order of the polymer segment length.[10] If the polymer cannot be adsorbed, then it will be excluded from the surface of the particles. Assuming the particles are large compared with the polymer, attractive particle−particle forces can arise through a mechanism of depletion.[3,4,6]

In earlier work,[1] we have shown that the flow properties of mesenchymal cell suspensions are extremely complex and that the addition of a biologically derived biomacromolecule (hyaluronic acid, HA) able to bind directly with the cells through defined cell surface receptors could change these properties, through the diminution of the adhesion strength and modification of the microstructure of the suspension and of the cellular aggregates. HA is a commonly used biomacromolecule in tissue engineering, as a component of hydrogels for cell encapsulation and delivery. However, besides HA, there are many other biomacromolecules used in tissue engineering, and not all of them have the ability to bind with specific receptors at the surface of cells.

This is the case for one of the most commonly used synthetic biomacromolecules, poly(ethylene glycol) (PEG). These molecules are obviously not naturally present in the body; however, they have received significant attention for the development of new tissue engineering scaffolds[11] for two main reasons. First, this polymer is relatively biologically inert and is well-tolerated *in vivo*.[12] Second, PEG molecules can be produced in a wide range of molecular weights and architectures, such as linear, branched, or star. Furthermore, they can be functionalized in variety of different ways, whether with functional chain end groups, proteins, peptides, growth factors, or other biochemical cues, to affect specific interactions with cells and other biomolecules.[13]

The scope of this study was thus to investigate the impact of the addition of branched PEG molecules, the most commonly utilized PEG variant in PEG-based tissue engineering scaffolds, displaying different end group functionalization (uncharged, negatively charged, and positively charged), on the rheology and flow behavior of a concentrated suspension of live cells of mesenchymal origin. Importantly, we performed this study over a wide range of cell concentrations and at a PEG concentration and molecular weight that are of direct relevance to those used in tissue engineering applications.[11]

MATERIAL AND METHODS

Sample Preparation. NIH-3T3 cells were cultured in high-glucose Dulbecco's modified Eagle's medium (DMEM) (Gibco, Invitrogen, USA) with 10% of fetal bovine serum (FBS) (Invitrogen, USA) and 1% penicillin/streptomycin (P/S) (Gibco, Invitrogen, USA) until they reached a confluence of 80% at 37 °C and 5% of CO_2. The cells were detached from their culture flask using trypLE (Gibco, Invitrogen, USA) and washed twice with 1 mL of phosphate buffered saline (PBS) (Amresco, USA). Once resuspended in a defined volume of suspending fluid, the volume fraction φ was measured using hematocrit capillaries, and the right amount of supernatant was removed to obtain the desired volume fraction. Different suspending fluids were prepared: the culture medium (DMEM (ionic strength 0.13 M), but without added FBS) with three different kinds of eight-arm PEGs of molecular weight 40, PEG, PEG-NH_2, and PEG-COOH (Jenkem Technology, USA), at a concentration of 40 mg/mL.

Rheology. Cell suspensions, with and without PEG polymers, were rheological characterized using an AR-G2 rheometer (TA Instruments, USA). Steady shear experiments were conducted at 20 °C under shear stress control. A cone-and-plate geometry (60 mm, 1°) was used to characterize the viscosity profile of the different suspending fluids. A parallel plate geometry was used to measure the viscosity of the cell suspensions as a function of shear stress, ensuring that a steady state was reached and verified. A solvent trap was used in order to prevent evaporation, the parallelism of the plates was checked using silicon oil according to an already extensively used protocol[14] before each experiment, and the systems were tested for slippage (as per our previous paper[1]) using protocol from Yoshimura and Prud'Homme.[15] All flow experiments were performed at shear stresses above 10^{-2} Pa in order to counteract the slow sedimentation process.[16−19]

Two-Photon Confocal Microscopy and Measurement of 3D Fractal Dimension. Once the cells were washed with PBS, as described above, the cells were resuspended in a defined volume of PBS with 1:1000 Hoescht (Invitrogen). They were then left at 37 °C for 30 min. The volume fraction was then determined and controlled as explained above. A known volume of supernatant was removed, and an equivalent volume of a solution of 8 mM of SulfoRhodamine B (SRB) was then added to the suspension in order to have a final concentration in SRB of 800 μM but with the volume fraction unchanged. A two-photon confocal microscope was used to take pictures at several heights at random points in the suspension under static conditions. The samples were illuminated at a wavelength of 850 nm, and emitted light was collected at 450−700 nm. Five pictures were taken at each height before being averaged. The contrast of the images was enhanced thanks to a pseudo flat-field filter, and the minimum and maximum of the brightness and contrast were set according to the histogram of the image. The images were then converted to binary, allowing the measurement of the actual volume fraction of the suspensions in addition to the size and shape of the cells. The fractal dimension of each of the suspensions was measured using a box counting method, as described previously.[1] All of these steps were performed using ImageJ (http://rsb.info.nih.gov/ij). We produced 3D reconstructions of the suspensions at rest, as shown in Figure 1, from which the fractal dimension of each of the suspensions at each volume fraction and PEG composition in 3D was measured. Several authors have previously shown that the size of an aggregate is proportional to the size of the particles constituting it.[20−22] It is therefore possible to connect the size of an aggregate (R_a), the number of particles in the aggregate (N), and its fractal dimension (d_f)

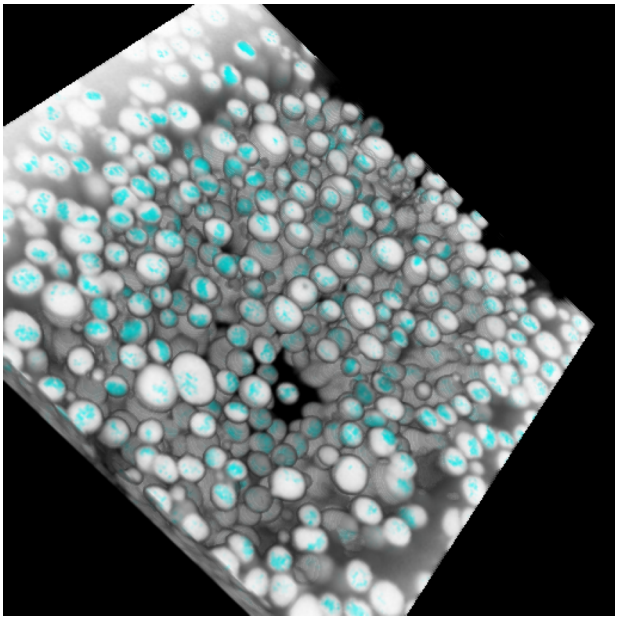

Figure 1. Example of a 3D reconstruction of a suspension of live cells from images taken with two-photon microscopy. Cells shown in this image are in the presence of PEG-NH_2 at a volume fraction of 50%.

$$\frac{R_a}{a} = N^{d_f} \tag{1}$$

where a is the radius of the constitutive particles. As shown previously, the average radius of fibroblast cells in suspension is 7.5 ± 1.7 μm.[1]

RESULTS

Rheology of Mesenchymal Cell Suspensions. The rheology of live mesenchymal cell suspensions in medium alone was studied and discussed in greater detail in our previous article.[1] However, for the sake of the latter discussion of the PEG-based systems, we will first outline the general trends exhibited by the cell suspension without PEG polymer added, the so-called DMEM-only system. As displayed in Figure 2, some noticeable characteristics can be observed (see the × symbols in Figure 2). First, at the lowest volume fraction tested (20%), the system exhibits a shear thinning zone, followed by a plateau, which is very similar in shape to that displayed by semidilute viscoelastic suspensions.[23] At volume fractions of 40 and 50%, the flow curves exhibit a pseudo plateau at moderate shear stresses that ends abruptly, with the viscosity dropping significantly at shear stresses of 1.7 and 4.6 Pa, respectively. This sharp restructuring of the material is followed by another Newtonian-like plateau, suggesting that the microstructure of the suspension does not evolve any further with increasing shear rate. At low shear stresses and high volume fractions, the suspension exhibits a yield stress, estimated using a Herschel–Bukley model to be approximately 0.35 and 1.5 Pa at volume fractions of 50 and 60%, respectively. For lower volume fractions, the presence of a yield stress is undetectable. As the shear increases, the material shows strong shear thinning, before reaching the pseudo Newtonian plateau mentioned above at volume fraction of 50%, indicating a reorganization of the material to a more stable microstructure. For the highest volume fraction (60%), the pseudo plateaus and the abrupt drop in viscosity are not observed, indicating a more continuous change in microstructure.

Rheology of Cell Suspensions with Different PEG Types. We have previously exemplified the ability of HA to adhere onto the surface of mesenchymal cells and significantly modify their rheological footprint.[1] PEG macromolecules are not known to adhere to cell surfaces through any defined interactions, for example, through receptor-mediated ligation. However, as depicted in Figure 2, their addition to these live cell suspensions still significantly modifies the rheology of the cell suspension. Furthermore, according to the charge of the end group on the eight-armed PEG molecules, the effects seem to vary greatly. These impacts also evolve with both the shear and volume fraction. The features of these curves include yield stress behavior, shear thinning, viscosity failure, and a Newtonian-like plateau. It can be easily appreciated that the presence of such complex rheological features for these concentrated cell–biomacromolecule suspensions will ultimately have significant implications when attempting to process them through an abrupt change in geometry, especially a contraction geometry, such as that experienced by any fluid at the exit of a syringe.

In order to discuss these complex behaviors, we will define three different shear regimes: the low shear regime, prior to the abrupt failure or viscosity decrease, the intermediate shear regime, at the abrupt failure, and the high shear regime, after the abrupt failure.

Low Shear Stresses. For low shear stresses, below the critical stress at which the viscosity decreases drastically, the differences in behavior between the different kinds of PEG is very noticeable, especially for PEG-NH_2. Indeed, at the lowest

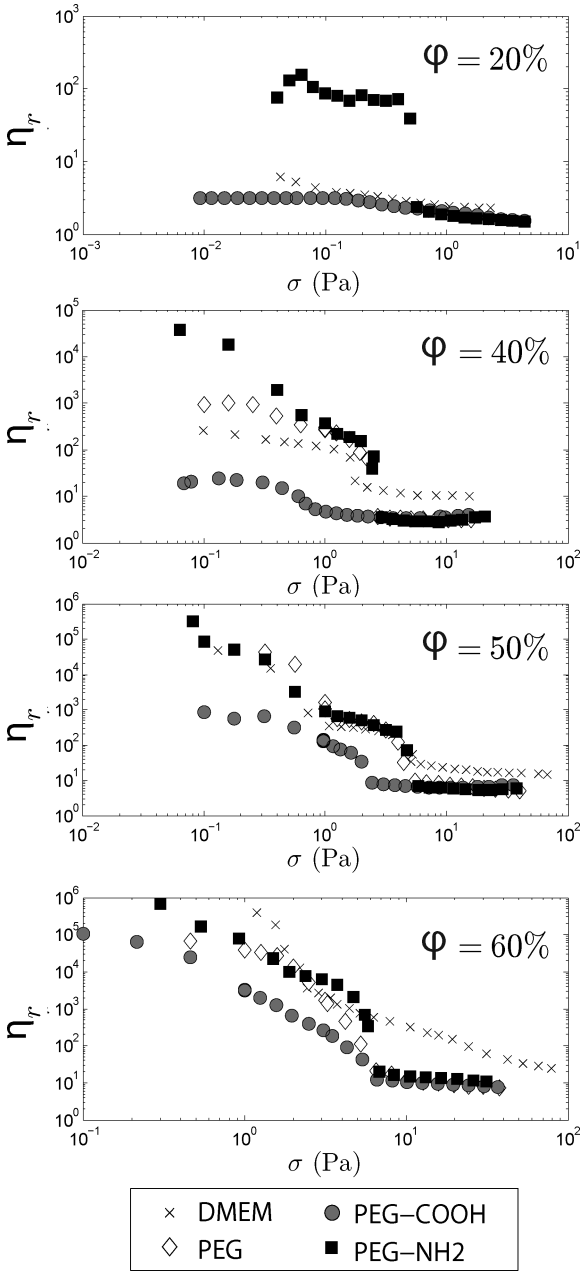

Figure 2. Relative viscosity as a function of shear stress for different PEG molecules at different volume fractions.

volume fraction of cells investigated (20%), the relative viscosity measured at small shear stresses for the suspension with PEG- NH_2 is roughly 30 times higher than that of any other system studied (DMEM, PEG, PEG-COOH). This increase in the relative viscosity with the addition of PEG-NH_2 is also observed for a volume fraction of 40%, with an associated increase of the yield stress at the lowest shear stresses tested. Interestingly, for higher volume fractions (at least 50%), the relative viscosity of the PEG-NH_2 system at low shear stresses more or less matches the behavior of the suspension with DMEM only. At a volume fraction of 60%, the yield stress for the PEG-NH_2 is now lower than that for the DMEM-only system.

Focusing next on the PEG-COOH system, the relative viscosity of this system is significantly lower than that of the suspension with only DMEM at volume fractions of 40, 50, and

dx.doi.org/10.1021/bm501481y | Biomacromolecules 2015, 16, 275–283

60%. This is less obvious at a volume fraction of 20%, except at shear stresses below 0.1 Pa. At very low shear stresses, the yield stress behavior is very nearly removed at volume fractions of both 40 and 50%. At 60%, a yield stress is still visible, but it is significantly attenuated.

The effect of the addition of PEG (without any charged end group, i.e., either the NH_2 or COOH group) is different again. At 20% volume fraction, the noncharged PEG system is similar to that of the PEG-COOH system. At a volume fraction of 40%, the relative viscosity at low shear stresses is slightly higher than that of DMEM only, but it is not as high as that for the PEG-NH_2 system. For a volume fraction of 50%, the relative viscosity of the suspension with noncharged PEG seems to be similar to that of the DMEM-only system. At 60%, the value of the relative viscosity of the noncharged PEG system at low shear stresses is lower than that with DMEM only and is of a magnitude similar to the PEG-NH_2 system.

From the analysis of the different systems used, it appears that several mechanisms are influencing the rheology of the suspension. At low shear stresses, these mechanisms are obviously linked with the charge of the PEG molecules used and evolve with the cell volume fraction. For the noncharged PEG and PEG-NH_2 systems in particular, the effects seem to diminish as the cell concentration approaches 60%.

Intermediate Shear Stresses. At the lowest volume fraction of cells investigated (20%), not only is the relative viscosity at small shear stresses with PEG-NH_2 significantly higher than that of any other system studied (DMEM, noncharged PEG, PEG-COOH) but also this is the only system at this volume fraction to display a critical shear stress at approximately 0.4 Pa.

For higher volumes fractions (40 and 50%), the behaviors of PEG-NH_2 and PEG are similar at intermediate shear stress values. At a volume fraction of 40%, the critical shear stress for each of these suspensions is approximately the same and slightly higher than that for the suspension with DMEM only. The relative viscosities of the PEG and PEG-NH_2 systems at 40% in this regime are also very similar, but they are higher than that of the DMEM-only system. At φ = 50%, the critical shear stress values are the same for the PEG, PEG-NH_2, and DMEM systems, and the relative viscosities of these three systems are almost identical.

At a volume fraction of 60%, however, the critical shear stress for the noncharged PEG system is now lower than that of the PEG-NH_2 system. In addition, no sharp change in viscosity is observed in the case of DMEM alone, so it is unclear if the critical shear stress for DMEM alone is higher or lower than that of the PEG or PEG-NH_2 system.

In this intermediate range of shear stresses, the behavior of the PEG-COOH system is significantly different from that of the other systems for most volume fractions above 20%. For volume fractions of 40 and 50%, the use of PEG-COOH significantly decreases the critical shear stress at which the viscosity drastically decreases. At 60%, it is hard to define a critical shear stress, as no abrupt change of slope in the relative viscosity profile is observed. The relative viscosities, at volume fractions of 40% and higher, are, however, clearly lower for the PEG-COOH system than that for the DMEM, PEG, or PEG-NH_2 system.

High Shear Stresses. After the rapid decrease in viscosity, there is very little difference between the noncharged PEG, PEG-COOH, and PEG-NH_2 systems, regardless of the volume fraction. The three systems exhibit a Newtonian-like plateau of similar relative viscosity. Interestingly, the relative viscosity of all of these PEG-cell systems is always lower than that of the DMEM alone−cell system, again regardless of volume fraction. The overlay of the three different kind of PEGs at high shear stresses indicates that this behavior is now independent of the charge of the PEG molecule, suggesting that it is induced only by the presence of dispersed PEG molecules throughout the suspension.

Measurements of the 3D Fractal Dimension of the Cell Suspension with the Addition of Different Types of PEG Molecules. The fractal dimension of each of the suspensions in the absence of shear in 3D was measured using two-photon confocal microscopy, as depicted in Figure 3.

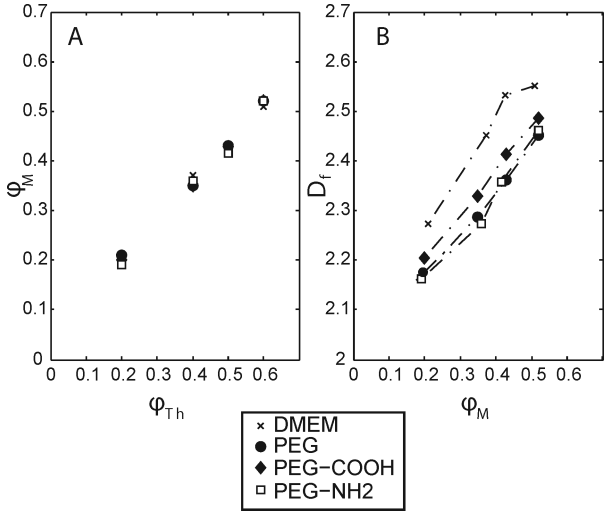

Figure 3. (A) Measured volume fraction as a function of the theoretical volume fraction. (B) Measured fractal dimension versus measured volume fraction.

The addition of PEG in the suspension, whatever its charge, decreases the fractal dimension. This trend is seen at any volume fraction. This result suggests that with the addition of PEG macromolecules the cell aggregates are more porous than that in a similar suspension without PEG. Focusing on the different types of PEG molecules investigated, the PEG-COOH system has the higher fractal dimension of the three types of PEG used. The addition of the noncharged PEG and PEG-NH_2 decreases the fractal dimension even further, but intriguingly, considering the significant differences in their rheological behavior, no definite distinction can be made between these two systems.

DISCUSSION

A common phenomenon occurring when biomacromolecules are added to a colloidal suspension is depletion.[3,4,6] Through the creation of concentration gradients of the added molecule, the overall impact on the suspension can be seen as the addition of an attractive force to the system. It is seen as an attractive force because the particles of the suspension will tend to be pushed together, with the macromolecules being excluded from the space between some of the particles, creating a concentration gradient and thus changing the osmotic pressure locally within the material.

PEG is a synthetic biomacromolecule that is not naturally present in the body. No specific PEG receptors are known to exist on the surface of mesenchymal cells and thus it is highly likely that the noncharged PEG molecules do not adhere

specifically to these cells. Characteristic signs of depletion behavior can be observed in Figure 2 when PEG is added at a volume fraction of 40% for shear stresses ranging from low to intermediate (up to the abrupt viscosity decrease). Indeed, depletion will effectively push the cells together, as depicted schematically in Figure 4A, which are adhesive to each other

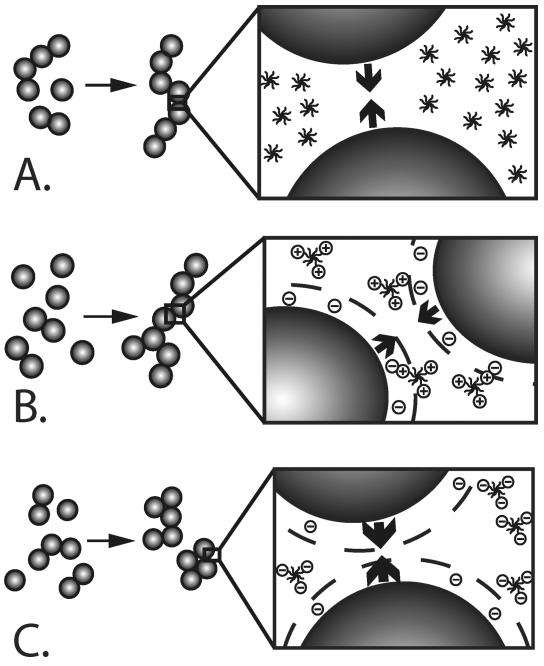

Figure 4. Schematic of the depletion in the suspension. (A) In the presence of PEG molecules: the PEG molecules are being excluded from the space between some of the particles, creating a concentration gradient, changing the osmotic pressure locally within the material and pushing the cells together. (B) In the presence of PEG-NH_2 molecules: PEG-NH_2 molecules counteracts the effects of depletion thanks to interactions with the peripheral pericellular matrix surrounding each of the cells. (C) In the presence of PEG-COOH molecules: the driving force for depletion is increased because of the presence of a significant number of dispersed negatively charged molecules.

through defined cell adhesion molecules at their surface, favoring the creation of a weak network and increasing the shear viscosity at low shear. However, once in contact, the adhesion strength between the cells is expected to be similar to the case of DMEM alone, as the same set of surface receptors is available. The critical shear stress (σ^*) should thus be similar for these two systems, as is confirmed in Figure 2 for volume fractions of 40 and 50%. This also shows that even if PEG, as an amphiliphilic molecule, can adsorb weakly and nonspecifically to hydrophobic cell surface proteins[24] it is clearly too weak to cause any changes in rheological footprint. At volume fractions of 50 and 60%, the low shear relative viscosity of the noncharged PEG system is also very similar to that measured in the DMEM-only system. This can be explained by the fact that at these higher volume fractions the cells are already in contact with each other and therefore depletion obviously does not play any significant role. The behavior at higher shear will be discussed later.

In the cases of the PEG-NH_2 or PEG-COOH systems, the charges introduced by the presence of the NH_2 or COOH end group on each arm of the eight-arm PEG could potentiate interactions with cell surfaces, albeit nonspecific, changing the flow behavior of the cell suspension system. It is quite difficult to quantitatively characterize the charge of a cell surface. However, the overwhelming majority of evidence suggests that cell surfaces are negatively charged, due to the cell membrane phospholipid's bilayer structure.[25] Indeed, it has been reported that the hydrophilic headgroup, present on the outer layer of the membrane, contains the negatively charged phosphate group.[26,27] In addition, cell surfaces are decorated with transmembrane proteins and also have pericellular bound extracellular matrix (ECM) proteins and fragments, even after trypsinization, which will influence the overall charge of the cell surface. The overall negative charge of many ECM molecules and most proteins on the cellular surface thus comforts us in viewing the mesenchymal cells studied here as negatively charged microparticles.[25,28]

Applying this assumption to the rheological data shown in Figure 2, it is possible to propose a mechanism for the observed influences of the charge of the added PEG polymer system on the rheology of the cell suspensions. In particular, it is possible to provide an explanation for the significant differences in behavior observed for the addition of PEG-NH_2 and PEG-COOH to these concentrated suspensions of live cells.

Under the pH condition tested (pH ~ 7.4), it is expected that the NH_2 group becomes a NH_3^+ group ($pK_a > 8$[29] or $pK_a > 9$[30]), and therefore is positively charged, and that the COOH group becomes a COO^- group ($pK_a < 5$[30]), and therefore is negatively charged.

With the surface of the cells assumed to be mainly electronegative, the charge of the NH_3^+ end group on each of the eight arms of the PEG molecule could counteract the effects of depletion expected for the noncharged PEG. Focusing first on the results at a volume fraction of 20%, the noticeable increase in the relative viscosity at low shear supports this proposed change in interaction within the system. Indeed, in a system where the concentration of cells is seemingly below that required to form a volume-spanning network, the attractive forces between the added molecules and the peripheral pericellular matrix surrounding each of the cells can induce the creation of a weak network, as shown schematically in Figure 4B. This weak network system now also exhibits a shear-induced breakdown, albeit at lower stresses than observed for higher volume fractions. At a volume fraction of 40%, the low shear relative viscosity is even higher than that of the neutral/noncharged PEG system. The yield stress is higher as well, suggesting an increase in network connectivity compared with that of the neutral PEG system. At 50 and 60%, the impact of PEG-NH_2 is similar to that of the neutral PEG system, likely due to there being so many cellular contacts in the system that override any differences in network structure imposed by these two types of PEG. At these higher volume fractions, the shear-induced breakdown also occurs at a similar critical shear stress for similar reasons. PEG-NH_2 does not change the set of receptors used to create strong adhesions between the cells but likely creates only additional weak contacts between the loose protein network on the outer periphery of the cells.

The PEG-COOH system displays completely different behavior to that of the other two PEG variants. Compared to the noncharged and positively charged PEG systems (and even the DMEM-only system), these suspensions always display a lower relative viscosity and, depending on the volume fraction, the absence of a lower critical stress, as shown in Figure 2. The critical shear stress is absent in this system until 50% volume fraction, and even then, it is also reduced compared to that of

the other systems. The yield stress is also significantly reduced at these higher volumes fractions. The fractal dimension also shows the smallest change (compared to the DMEM-only system) for all PEG systems investigated (Figure 3), suggesting that there are some minor structural rearrangements as a result of this negatively charge PEG that differ from the PEG and PEG-NH_2 systems.

There are two possible mechanisms that may be driving such behavior. First, assuming that these cells are globally negatively charged, a highly negatively charged eight-arm PEG may be repulsed by the cell surface. In this case, the presence of a significant number of dispersed negatively charged molecules will increase the driving force for depletion throughout the system and thus discourage the formation of a volume spanning network, as in the case of the other systems at 40%, and promote the formation of dispersed, large, denser cellular aggregates or flocs, as depicted in Figure 4C. However, as volume fraction increases, these aggregates begin to make contact, and a spanning network is formed. Even so, given the difference in the network connectivity, we would then expect the appearance of lower yield stresses and critical shear stresses compared to that in the other systems, as is observed.

Alternatively, another valid proposition would be that, given the differences in size between the cells (tens of micrometers) and the PEG molecules (tens of nanometers), short-range interactions will occur between the positively charge cell surface bound proteins (or positively charged domains thereof) and the PEG-COOH molecules. This would allow the polymer to bind within the pericellular protein layer while not binding explicitly to the cell membrane surface. These interactions would be short-range and diffuse within the cell surface bound protein layer. These interactions between the PEG-COOH and the pericellular proteins would compact or condense the pericellular protein coat, obscure the cell surface receptors involved in cellular adhesion, and hence reduce cell−cell adhesion strength, as depicted in Figure 5. Aggregates would thus still be able to be created and would be denser than those created in the presence of the other kinds of PEG molecules, as suggested by the values of the fractal dimension for the PEG-COOH system being slightly higher than those for the PEG and PEG-NH_2 systems. In all likelihood, both mechanisms are probably at play in this complex system; however, without further experimental evidence to support either of these proposed mechanisms of action of the PEG-COOH, the exact mechanism remains to be elucidated.

For all PEG systems, regardless of charge, when the shear stress is higher than the critical shear stress, another mechanism seems to be at play. Indeed, the relative viscosities of the three PEG systems collapsed onto one another and are lower than the relative viscosity of the cell suspension with just DMEM. As discussed above, the different types of PEG molecules have different impacts on the rheology of the suspension, according to their charge and therefore according to how they interact with the cells. Because of this collapse at higher shear stresses, the mechanism at high shear stresses appears to be independent of the charge and therefore can be imputed to the presence of the PEG molecules alone. It is likely that the presence of the PEG molecules in some way reduces the transient contacts between cells that occur when the suspension is sheared (schematic in Figure 6), acting like a lubricant to the system.

Using a simple analytical model developed in a previous paper,[1] we estimated the adhesion force between cells in these suspensions.

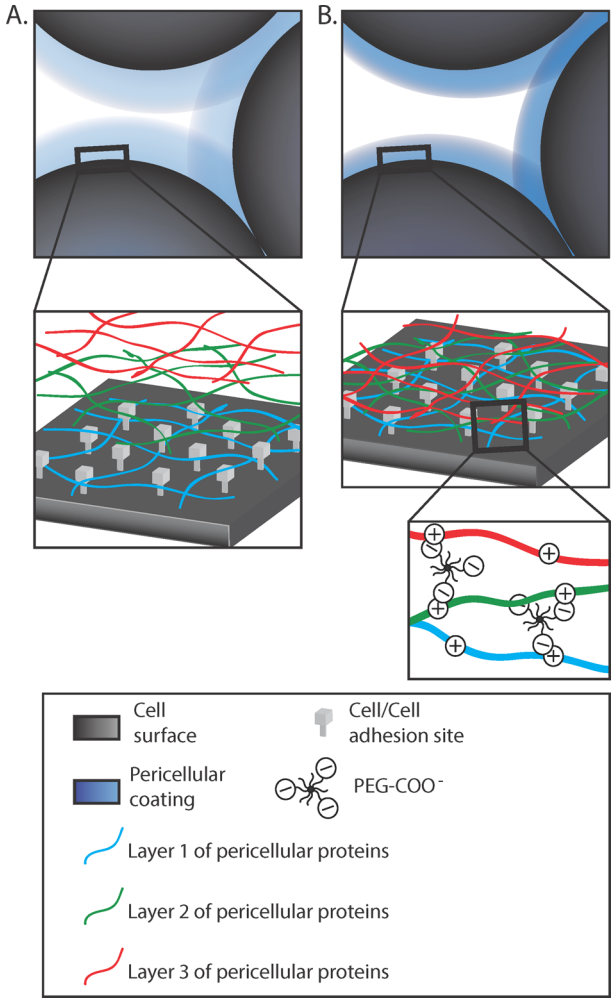

Figure 5. Schematic of the effect of PEG-COOH. Pericellular proteins compact or condense the pericellular protein coat, obscure the cell surface receptors involved in cellular adhesion, and hence reduce cell−cell adhesion strength: (A) without PEG-COOH and (B) in the presence of PEG-COOH. The presence of PEG-COOH links the different layers of pericellular proteins, therefore inducing a denser pericellular protein coat.

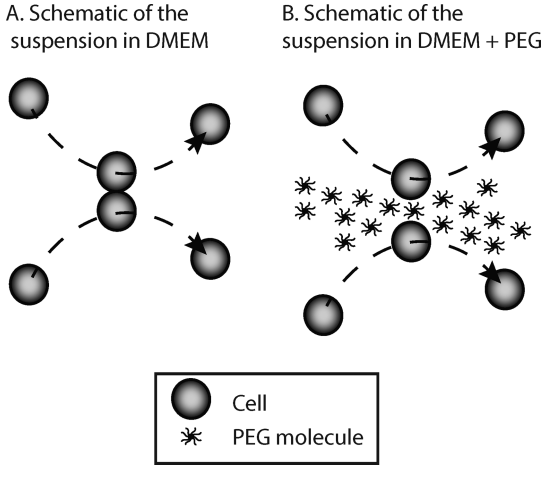

Figure 6. (A) Schematic of the suspension in DMEM alone, at shear stresses higher than the critical shear stress. (B) Schematic of the suspension in DMEM + PEG, at shear stresses higher than the critical shear stress.

dx.doi.org/10.1021/bm501481y | *Biomacromolecules* 2015, 16, 275−283

In suspension rheology, several sets of equations can be used to model the flow behavior of such systems. A widely used model is the Krieger−Dougherty equation

$$\eta_r = \left(1 - \frac{\varphi}{\varphi_0}\right)^{-[\eta]\varphi_0} \tag{2}$$

where η_r is the relative viscosity, φ_0 is the maximum packing volume fraction, $[\eta]$ is the intrinsic viscosity, and φ is the volume fraction. As stated earlier in this article, cells have the ability to bind and create large cellular aggregates within which the suspending fluid can be trapped. As a consequence, the effective volume fraction of the system is not strictly equal to the cell volume fraction but instead must take trapped fluid into account. To do so, the effective volume fraction was defined as the product between the regular volume fraction and a packing factor φ^*

$$\varphi_A = \varphi\varphi^* \tag{3}$$

Consequently, the effective volume fraction changes as the aggregates get broken down with the application of shear, and this is dependent on the geometrical characteristics of the aggregates, such as the fractal dimension d_f[1,31]

$$\varphi^* = \left(1 + \left(\frac{\sigma^*}{\sigma}\right)^m\right)^{3-d_f} \tag{4}$$

where σ is the applied shear stress, σ^* is a critical shear stress linked to the adhesion energy per surface units, and m is a parameter that depends on the reversibility of the deformation experienced by the aggregates.[32,33] Injecting the effective volume fraction φ_A in the Krieger−Dougherty model, the governing equation relating the reduced viscosity to the volume fraction of the suspension at a defined shear stress becomes

$$\eta_r = \left(1 - \frac{\varphi}{\varphi_0}\left(1 + \left(\frac{\sigma^*}{\sigma}\right)^m\right)^{3-d_f}\right)^{-[\eta]\varphi_0} \tag{5}$$

The results of the rheometrical study and those derived from the two-photon confocal measurements mean that for the suspensions investigated in this work there is only one unknown parameter within eq 5, that being the parameter σ^*. This parameter is linked to the adhesion energy per surface units and hence, by solving this equation, it is therefore possible to estimate the adhesion force between individual cells using a simple Derjaguin approximation[1,31,34]

$$F^* \approx \sigma^* a^2 \tag{6}$$

where a is the radius of a cell.

Using this set of equations, a master curve-like plot of the relative viscosity versus the effective volume fraction can be created for all of the systems investigated (Figure 7). The values of the fractal dimensions input into the model were those measured from the two-photon confocal microscope images for each PEG system under static conditions (Figure 3).

The value of the critical shear stress σ^* for the systems with DMEM was found to be equal to 0.65 Pa. This represents an adhesion force of 36.5 pN, which is in agreement with the values reported in the literature, which range from 15 to 40 for mouse fibroblast Balb/c3T3 and up to 48 for WM115 melanoma cells.[35−37] Once validating the coherence of the model, the data from the other systems can be used in a similar manner. For the systems with PEG and PEG-NH_2, the critical

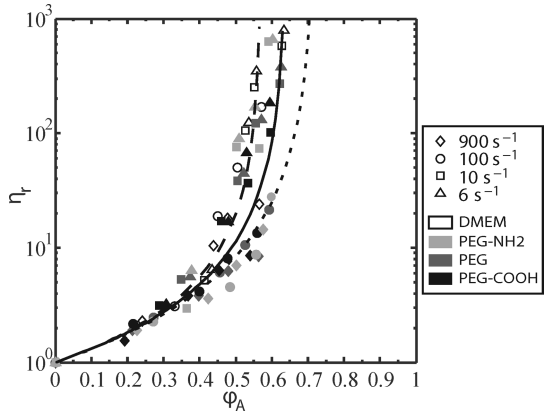

Figure 7. Relative viscosity as a function of the effective volume fraction for different PEG molecules and for different shear rates. The solid line is the Krieger and Dougherty model with φ_0 = 0.64, the broken line is the Krieger and Dougherty model with φ_0 = 0.57, and the dotted line is the Krieger and Dougherty model with φ_0 = 0.72.

shear stress was found to be the same as that for the DMEM system. This is in agreement with the fact that the shear stresses at which the viscosity drops drastically in Figure 2 are the same for these three systems. This confirms that the differences observed among the flow curves of these three systems are not related to a modification in the strength of cellular adhesions but to a modification of the dynamics of the formation of the aggregates, as proposed in Figure 4A,B.

For the PEG-COOH system, however, σ^* had to be set equal to 0.05 Pa in order to collapse the data points onto the mastercurves, indicating an adhesion strength of 2.8 pN. The adhesion force of the PEG-COOH system is therefore considerably lower than that for the other systems, as suggested by the different rheological footprint for this system (Figure 2). This result supports the proposed the mechanism depicted in Figure 5, where cell surface receptors involved in cellular adhesion are obscured by the interactions between PEG-COOH and the pericellular proteins. The alternative mechanism depicted in Figure 4C is not, however, invalidated by this result, as the depletion effects may still occur in concert with the mechanism shown in Figure 5.

Interestingly, further inspection of the data in Figure 7 shows that the data for all PEG systems for the highest shear stresses do not seem to collapse on the Krieger−Dougherty model with φ_0 = 0.64, but onto a curve using φ_0 = 0.72. Even though a part of this deviation is likely due to the deformability of the cells, it is more significant when PEG is present compared to that with DMEM only, indicating other contributions to this behavior. These contributions are likely due to differences in the microscopic arrangement of the suspensions and of the molecules under such shearing conditions. In an attempt to explain the low relative viscosities at these high shear stresses, we have previously stated that the presence of PEG molecules in these solutions at such concentrations likely prevents the brief adhesion between neighboring cells under high shear. We thus took σ^* equal to 0 for shear stresses higher than the intermediate range (i.e., past the abrupt decrease in viscosity) for the PEG systems, and, intriguingly, we found that the data collapsed once more on the Krieger−Dougherty model with φ_0 = 0.64, as displayed in Figure 8. Even though enticing to believe, having an adhesion force strictly equal to 0 hardly makes any real physical sense. It is therefore difficult to

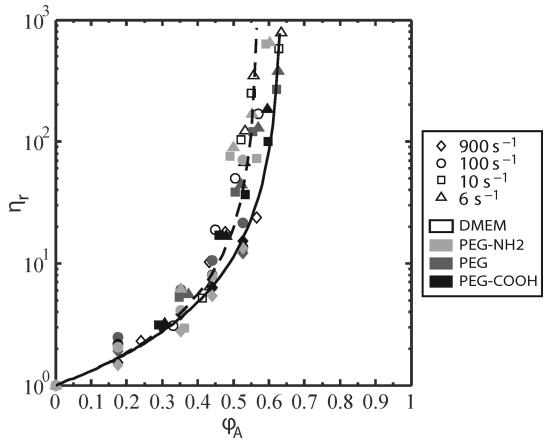

Figure 8. Relative viscosity as a function of the effective volume fraction for different PEG molecules and for different shear rates but with the value of σ^* equal to 0 for the PEG systems for high shear stresses (beyond abrupt decrease in viscosity). The solid line is the Krieger and Dougherty model with $\varphi_0 = 0.64$; the broken line is the Krieger and Dougherty model with $\varphi_0 = 0.57$.

absolutely confirm the suggested hypothesis for such high shear stress behavior, as both a change in adhesion strength and/or a change in the microscopic conformation may be the origin of the differences observed between the PEG systems and the DMEM-only system. This is especially true when taking into account that a change in adhesion force often leads to a different microscopic reorganization. Further experiments tracking and imaging, with fluorescently labeled PEG, cell membranes and pericellular proteins are required to provide the required insight into these complicated interactions and such multicomponent systems.

CONCLUSIONS

Mesenchymal cell suspensions are the base material of many tissue engineering and regenerative medicine approaches to tissue repair, and they are often combined with synthetic polymers as carriers or encapsulation systems prior to injection into sites of tissue damage. The understanding and knowledge of the behavior of these living systems in a processing framework, for example, under flows and shear stresses applicable to syringe-based injection, are thus central to their use and ultimately to the viability of the cells post such a process. The data presented in this article confirms the importance of understanding the impacts of the addition of biomacromolecules on the flow properties of live cell suspensions. Even if the added biomacromolecules lack the ability to bind directly with cell surface receptors, a change in composition of the suspending fluid can have drastic impacts on the rheology of the live cell suspension, whether they are due to depletion at low shear or due to modification of the transient dynamics of cells in contact with each other. Even small changes to the physicochemical properties of the added molecules, such as the charge of these molecules, cannot be neglected. Indeed, compared to a suspension of cells alone, the addition of macromolecules of varying charge and at concentrations often employed in tissue engineering practices can either increase or decrease the yield stress behavior, modulate shear thinning behavior, and introduce or eradicate abrupt rupture of the suspension under shear, therefore making the cell suspension harder or easier to process through a syringe, a common delivery method for cellular therapies.

AUTHOR INFORMATION

Corresponding Author

*E-mail: j.cooperwhite@uq.edu.au.

Notes

The authors declare no competing financial interest.

ACKNOWLEDGMENTS

This research was supported by an Australian Research Council Discovery grant (no. DP1095429), by the University Joseph Fourier, and partly by the Région Rhône-Alpes.

REFERENCES

(1) Maisonneuve, B.; Roux, D.; Thorn, P.; Cooper-White, J. *Biomacromolecules* **2013**, *14*, 4388−4397.
(2) Zoro, B.; Owen, S.; Drake, R.; M, C. M.; Hoare. *Biotechnol. Bioeng.* **2009**, *103*, 1236−1247.
(3) Hunter, R. *Foundations of Colloid Science*; Clarendon Press: Oxford, 1992.
(4) Israelachvili, J. *Intermolecular and Surface Forces*; Academic Press: London, 1997.
(5) Quemada, D.; Berli, C. *Adv. Colloid Interface Sci.* **2002**, *98*, 51−85.
(6) Russel, W.; Saville, D.; Schowalter, W. *Colloidal Dispersions*, 2nd ed.; Cambridge University Press: New York, 1991.
(7) Napper, D. *J. Colloid Interface Sci.* **1977**, *58*, 390−407.
(8) Vincent, B. *Adv. Colloid Interface Sci.* **1974**, *4*, 193−277.
(9) Flory, P. *Principles of Polymer Chemistry*; Cornell University Press: Ithaca, NY, 1953.
(10) Ji, H.; Hone, D.; Pincus, P.; Rossi, G. *Macromolecules* **1990**, *23*, 698−707.
(11) Menzies, D.; Cameron, A.; Munro, T.; Wolvetang, E.; Grondahl, L.; Cooper-White, J. *Biomacromolecules* **2013**, *14*, 413−423.
(12) Hutson, C.; Nichol, J.; Aubin, H.; Bae, H.; Yamanlar, S.; Al-Haque, S.; Koshy, S.; Khademhosseini, A. *Tissue Eng., Part A* **2011**, *17*, 1713−1723.
(13) DeLong, S.; Gobin, A.; West, J. *J. Controlled Release* **2005**, *109*, 139−148.
(14) Kramer, J.; Uhl, J.; Prudhomme, R. *Polym. Eng. Sci.* **1987**, *27*, 598−602.
(15) Yoshimura, A.; Prud'Homme, R. *J. Rheol.* **1988**, *32*, 53−67.
(16) Acrivos, A.; Fan, X.; Mauri, R. *J. Rheol.* **1994**, *38*, 1285−1296.
(17) Chapman, B.; Leighton, D. *Int. J. Multiphase Flow* **1991**, *17*, 469−483.
(18) Eckstein, E.; Bailey, D.; Shapiro, A. *J. Fluid Mech.* **1977**, *79*, 191−208.
(19) Leighton, D.; Acrivos, A. *Chem. Eng. Sci.* **1986**, *41*, 1377−1384.
(20) Iordan, A.; Duperray, A.; Verdier, C. *Phys. Rev. E* **2008**, *77*, 011911 .
(21) Boynard, M.; Haïder, L.; Snabre, P. *ITBM-RBM* **2002**, *23*, 23−39.
(22) de Gennes, P. *Scaling Concepts in Polymer Physics*; Cornell University Press: Ithaca, NY, 1979.
(23) Snabre, P.; Mills, P. *Colloids Surf., A* **1999**, *152*, 79−88.
(24) Wu, J.; Wang, Z.; Lin, W.; Chen, S. *Acta Biomater.* **2013**, *9*, 6414−6420.
(25) Goldenberg, N.; Steinberg, B. *Cancer Res.* **2010**, *70*, 1277−1280.
(26) Alberts, B.; Johnson, A.; Lewis, J.; Raff, M.; Roberts, K.; Walter, P. *Molecular Biology of the Cell*, 4th ed.; Garland Science: New York, 2002.
(27) Cooper, G. *The Cell: A Molecular Approach*, 2nd ed.; Sinauer Associates: Sunderland, MA, 2000.
(28) Sorokin, L. *Nat. Rev. Immunol.* **2010**, *10*, 712−723.
(29) Kinstler, O.; Brems, D.; Lauren, S.; Paige, A.; Hamburger, J.; Treuheit, M. *Pharm. Res.* **1996**, *13*, 996−1002.
(30) Ryman-Rasmussen, J.; Riviere, J.; Monteiro-Riviere, N. *Toxicol. Sci.* **2006**, *91*, 159−165.
(31) Snabre, P.; Mills, P. *J. Phys. III* **1996**, *6*, 1811−1834.
(32) Potanin, A. *J. Colloid Interface Sci.* **1993**, *157*, 399−410.

(33) Bossis, G.; Meunier, A. *J. Chem. Phys.* **1991**, *94*, 5064−5070.
(34) Derjaguin, B.; Muller, V.; Toporov, Y. *J. Colloid Interface Sci.* **1975**, *53*, 314−326.
(35) Puech, P.; Poole, K.; Knebel, D.; Muller, D. *Ultramicroscopy* **2006**, *106*, 637−644.
(36) Zhang, X.; Chen, A.; Leon, D.; Li, H.; Noiri, E.; Moy, V.; Goligorsky, M. *Am. J. Physiol.: Heart Circ. Physiol.* **2003**, *286*, H359−H367.
(37) Sirghi, L.; Ponti, J.; Broggi, F.; Rossi, F. *Eur. Biophys. J.* **2008**, *37*, 935−945.